Development 134, 1499-1508 (2007) doi:10.1242/dev.02829

Lack of the murine homeobox gene *Hesx1* leads to a posterior transformation of the anterior forebrain

Cynthia L. Andoniadou[1], Massimo Signore[1], Ezat Sajedi[1], Carles Gaston-Massuet[1], Daniel Kelberman[2], Alan J. Burns[1], Nobue Itasaki[3], Mehul Dattani[2] and Juan Pedro Martinez-Barbera[1,*]

The homeobox gene *Hesx1* is an essential repressor that is required within the anterior neural plate for normal forebrain development in mouse and humans. Combining genetic cell labelling and marker analyses, we demonstrate that the absence of *Hesx1* leads to a posterior transformation of the anterior forebrain (AFB) during mouse development. Our data suggest that the mechanism underlying this transformation is the ectopic activation of Wnt/β-catenin signalling within the *Hesx1* expression domain in the AFB. When ectopically expressed in the developing mouse embryo, *Hesx1* alone cannot alter the normal fate of posterior neural tissue. However, conditional expression of *Hesx1* within the AFB can rescue the forebrain defects observed in the *Hesx1* mutants. The results presented here provide new insights into the function of *Hesx1* in forebrain formation.

KEY WORDS: Mouse, *Hesx1*, Anterior forebrain, Wnt, β-catenin, Cre, Rosa26

INTRODUCTION

The homeobox gene *Hesx1* is a member of the paired-like family of homeobox proteins and functions as a transcriptional repressor (Thomas et al., 1995; Hermesz et al., 1996; Dasen et al., 2001). *Hesx1* and its orthologues in other vertebrates (Anf genes) are expressed in the rostral region of the embryo during gastrulation and neurulation in all species analysed (Hermesz et al., 1996; Thomas and Beddington, 1996; Kazanskaya et al., 1997; Knoetgen et al., 1999). In mouse, *Hesx1* expression is very dynamic, and *Hesx1* transcripts are detected in anterior regions of the visceral endoderm, definitive endoderm and neural ectoderm during early development. Later, *Hesx1* expression is restricted to the Rathke's pouch.

Hesx1-deficient embryos show a reduction in anterior forebrain (AFB) tissue rostral to the zona limitans intrathalamica (ZLI) at 8.5 dpc. The presumptive AFB is initially induced, but this territory is reduced at a later stage of development in *Hesx1*$^{-/-}$ mutants. Chimeric analysis has shown that this forebrain phenotype is a consequence of the requirement of *Hesx1* within the anterior neural ectoderm, and not due to disturbances in the anterior visceral endoderm or anterior definitive endoderm (Martinez-Barbera et al., 2000). *Hesx1* mutants also show defects in dorsal forebrain commissural structures, eye abnormalities and pituitary dysplasia (Dattani et al., 1998). A comparable phenotype is observed in a human congenital disorder called septo-optic dysplasia (SOD). Indeed, mutations in *HESX1* are associated with familial cases of SOD and other forms of hypopituitarism in humans (Dattani et al., 1998; Dattani, 2004; Sobrier et al., 2006). In *Xenopus*, overexpression of the *Hesx1* orthologue, *Xanf1*, results in enlargement of the neural plate (NP) at the expense of epidermis and neural crest (NC) (Ermakova et al., 1999). Thus, it is now established that *Hesx1* is essential for normal AFB development in vertebrates. However, little is known about how *Hesx1* performs its function.

[1]Neural Development Unit and [2]Biochemistry, Endocrinology and Metabolism Unit, UCL-Institute of Child Health, 30 Guilford Street, WC1N 1EH, London, UK. [3]National Institute for Medical Research, The Ridgeway, Mill Hill, NW7 1AA, London, UK.

*Author for correspondence (e-mail: j.martinez-barbera@ich.ucl.ac.uk)

Accepted 5 February 2007

Experiments in *Xenopus*, zebrafish, chick and mammals have provided compelling evidence indicating that suppression of posteriorising signals is an essential requisite for the formation of anterior neural tissue (Kimura et al., 2000; Perea-Gomez et al., 2001; Kudoh et al., 2002; Wilson and Houart, 2004; Stern, 2005). Among them, the Wnt/β-catenin pathway plays a key role in anterior-posterior patterning of the NP [(Yamaguchi, 2001; Wilson and Houart, 2004; Marikawa, 2006) and references therein]. It is thought that the action of Wnt signalling inhibitors and activators create a gradient along the neural ectoderm (high caudally and low rostrally) that is required for normal anterior-posterior regionalisation of the NP in distinct subdivisions (Leyns et al., 1997; Glinka et al., 1998; Hsieh et al., 1999; Kiecker and Niehrs, 2001; Nordstrom et al., 2002). Normal AFB development is particularly sensitive to Wnt/β-catenin signalling (Fredieu et al., 1997; van de Water et al., 2001; Houart et al., 2002). For instance, the zebrafish masterblind mutants, which carry a mutation in Axin1 that abolishes binding to Gsk3β causing Wnt/β-catenin signalling overactivation, show a phenotype in which telencephalon and eyes are reduced or absent, and dorsal diencephalic fates are expanded rostrally (van de Water et al., 2001; Heisenberg et al., 2001). Similarly, lack of *Tcf3/Headless* repressor function leads to the loss of anterior neural tissue (Kim et al., 2000). In chick, it has been shown that posterior forebrain character can be induced in explants, which would normally acquire an AFB fate, through the direct caudalising activity of Wnt proteins (Nordstrom et al., 2002). In mouse, both overexpression of *Wnt8* and lack of Wnt/β-catenin antagonists lead to suppression of anterior neural fates (Popperl et al., 1997; Mukhopadhyay et al., 2001; Satoh et al., 2004). Therefore, it is now established that Wnt/β-catenin signalling must be modulated during vertebrate development to allow normal anterior-posterior patterning of the NP; in particular, Wnt/β-catenin signalling needs to be suppressed for the AFB to develop.

The transcriptional repressors *Hesx1*, *Six3* and *Rax* (*Rx*) show overlapping expression patterns in the anterior neural ectoderm during early mouse development (Oliver et al., 1995; Thomas and Beddington, 1996; Mathers et al., 1997). Moreover, *Six3* and *Rax* mutants show defects in the forebrain, such as reduced telencephalon and eyes, which are very similar to those observed

in *Hesx1*$^{-/-}$ mutants (Mathers et al., 1997; Martinez-Barbera et al., 2000; Lagutin et al., 2003). A mechanism has been postulated in which *Six3* is thought to directly repress the *Wnt1* promoter and thereby reduce Wnt/β-catenin signalling in the AFB. Whether or not *Hesx1* and *Rax* perform a similar function during forebrain formation is an important question that remains unanswered.

To further understand the function of *Hesx1* in forebrain development, we have analysed in detail the neural patterning of *Hesx1* mutant embryos and performed a genetic fate map of *Hesx1*-expressing cells in normal embryos and *Hesx1* homozygous mutants. Our data indicate that in the absence of *Hesx1* there is a posterior transformation of the AFB. Contrary to the observations in the *Six3* mutants, HESX1 appears not to directly repress the *Wnt1* locus, although absence of *Hesx1* leads to an anteriorisation of *Wnt1* expression and ectopic activation of the Wnt/β-catenin targets *Sp5* and *Axin2* in the AFB. Gain-of-function experiments suggest that *Hesx1* alone cannot anteriorise posterior neural tissue, but can rescue the forebrain defects of the *Hesx1*-deficient mutants.

MATERIALS AND METHODS

Generation of the *Hesx1*$^{Cre/+}$ mouse line

The *Hesx1-Cre* targeting vector was generated by replacing the *Hesx1* coding region with *Cre* recombinase (Fig. 4). CCE embryonic stem cells (129/SvEv) (kindly provided by E. Robertson, Wellcome Trust Centre for Human Genetics, Oxford, UK) were electroporated and 500 colonies were picked, expanded and screened as described (Dattani et al., 1998). Two correctly targeted clones were isolated and injected into blastocysts from C57BL/6J mice. The *PGK-Neo* cassette was excised by crossing heterozygous mice with the ACTB:FLPe strain (Rodriguez et al., 2000). *Hesx1*$^{Cre/+}$ mice were maintained on the C57BL/6J background and to date have been backcrossed a total of eight times. *Hesx1*$^{Cre/Cre}$ embryos showed the forebrain and pituitary defects observed in *Hesx1*$^{-/-}$ mutants. It is worth noting that the severity of the phenotype of the *Hesx1*-deficient embryos (*Hesx1*$^{Cre/Cre}$ and *Hesx1*$^{-/-}$) has increased compared with the initial analysis (Dattani et al., 1998). No viable homozygous mice are now identified at weaning and eye defects are fully penetrant with variable expressivity. We think this is a consequence of maintaining the colony on the C57BL/6J, whereas it was previously kept on a C57BL/6 inbred colony maintained at the National Institute for Medical Research, UK.

Generation of the *R26*$^{Cond\text{-}Hesx1/+}$ mouse line

The components of the *Rosa26* (*R26*) targeting vectors were a gift (Soriano, 1999; Srinivas et al., 2001). To avoid possible interference with the translation of *Hesx1* owing to the presence of an ATG within the *loxP* sites, we generated a *pBigT-invloxP* by inverting the orientation of both *loxP* sites (Ivanova et al., 2005). After electroporation, a total of 300 clones were picked, expanded and frozen (see Fig. S6 in the supplementary material). Five correctly targeted clones were identified and two were used for blastocyst injection (C57BL/6J background). *R26*$^{Cond\text{-}Hesx1/+}$ heterozygous mice were backcrossed three times with C57BL/6J mice and then intercrossed to generate *R26*$^{Cond\text{-}Hesx1/Cond\text{-}Hesx1}$ homozygous mice, all of which were viable and fertile.

Genetic crosses

Hesx1$^{Cre/+}$mice were crossed with *R26*$^{Cond\text{-}lacZ/Cond\text{-}lacZ}$ reporter animals to generate the *Hesx1*$^{Cre/+}$;*R26*$^{Cond\text{-}lacZ/+}$ compound mice, then backcrossed to *R26*$^{Cond\text{-}lacZ/Cond\text{-}lacZ}$ mice to obtain *Hesx1*$^{Cre/+}$;*R26*$^{Cond\text{-}lacZ/Cond\text{-}lacZ}$ mice and embryos. *Hesx1*$^{Cre/+}$;*R26*$^{Cond\text{-}lacZ/+}$ and *Hesx1*$^{Cre/-}$;*R26*$^{Cond\text{-}lacZ/+}$ embryos were generated from crosses between *Hesx1*$^{Cre/+}$;*R26*$^{Cond\text{-}lacZ/Cond\text{-}lacZ}$ and *Hesx1*$^{+/-}$ mice. *Hesx1*$^{+/-}$ mice carry a null allele and have been described previously (Dattani et al., 1998).

Genotyping of mice and embryos

Embryos and neonates were genotyped by PCR on DNA samples prepared from tail tips, yolk sacs or whole embryos. Primer sequences and PCR protocols are available on request.

Histology, X-Gal staining, in situ hybridisation (ISH), TUNEL staining and cell proliferation

Histology, X-Gal staining, TUNEL staining and ISH were performed as described (Martinez-Barbera et al., 2002). Proliferation was assessed using the anti-phospho-histone H3 antibody (mitosis marker; Upstate Biotechnology). Three embryos of each genotype at similar developmental stages were embedded in wax and sectioned. Immunostaining was performed following standard procedures and sections were counterstained with DAPI. For analysis, a total of over 5,000 nuclei were counted from matching sections containing forebrain tissue. The mitotic index was expressed as a percentage of mitotic nuclei from the total number of nuclei.

EMSA, cell transfections, luciferase assays and western blots

EMSA was performed as previously described (Dattani et al., 1998). DNA transfections were carried out in CHO and 293 cells as described (Brickman et al., 2001) using reporter plasmids encompassing specific regions of the *Wnt1* locus containing putative *Hesx1*-binding sites. The western blot for HESX1 used a specific rabbit serum we have generated.

qRT-PCR and RT-PCR analysis

Total RNA was isolated from embryos using the RNeasy Micro Kit (Qiagen). First-strand cDNA synthesis was performed using the Omniscript RT Kit (Qiagen) according to the manufacturer's recommendations. Amplification of *Hesx1*, *Cre* and *Gapdh* (endogenous control) with specific primers was performed using SYBRGreenER (Invitrogen) on an ABI 7500 Real-Time PCR machine (Applied Biosystems) and analysed using the ABI system software. For RT-PCR analysis, specific primers for *Hesx1*, *Cre* and *Gapdh* were used to amplify cDNA templates from RNA extracted from whole embryos or specific regions of the neural tube using Trizol (Invitrogen). Primer sequences and PCR conditions are available on request.

RESULTS

Posterior transformation of AFB in *Hesx1*-deficient embryos

We have previously shown that in the absence of *Hesx1* there is a lack of AFB tissue at 8.5 dpc, but the reasons underlying this phenotype are not known (Martinez-Barbera et al., 2000). To find out the cellular basis of the early forebrain defects, we analysed neural patterning, proliferation and apoptosis of *Hesx1*$^{-/-}$ in comparison with *Hesx1*$^{+/-}$ and wild-type embryos from 7.5 to 9.5 dpc.

At presomitic stages, the expression domains of *Six3* (AFB marker), *Atx* (*Dmbx1*) and *Pax2* (posterior forebrain and midbrain markers at these stages), and *Hoxb1* (hindbrain marker) were identical in all genotypes (Fig. 1A,B and data not shown) (Oliver et al., 1995; Nornes et al., 1990; Hunt and Krumlauf, 1991; Gogoi et al., 2002). At the 0- to 1-somite stage, *Pax6* is expressed in the prospective forebrain region of the developing mouse embryo (Walther and Gruss, 1991). *Pax6* expression in the anterior NP was significantly reduced in *Hesx1*$^{-/-}$ mutants when compared with *Hesx1*$^{+/-}$ or wild-type littermates at this stage, thus confirming that the prospective forebrain region is reduced only at the early somite stage (Fig. 1C) (Martinez-Barbera et al., 2000). The possibility that prospective forebrain was being respecified was analysed using the neural crest (NC) markers *Pax3* and *Foxd3*. These markers are expressed on the margin of the anterior NP at the 2- to 3-somite stage in wild-type embryos, but the most rostral region is free of *Pax3* and *Foxd3* transcripts (Fig. 1D,F,H,J) (Goulding et al., 1991; Labosky and Kaestner, 1998). By contrast, their expression domains were anteriorised in the 2- to 3-somite stage *Hesx1*$^{-/-}$ mutants, and the region devoid of *Pax3* and *Foxd3* expression was clearly reduced when compared with *Hesx1*$^{+/-}$ or wild-type embryos (Fig. 1E,G,I,K). It is important to note that these changes were observed prior to a gross lack of neural tissue, although there was a slight change in the shape of the anterior NP (Figs 1 and 2; see below). NC

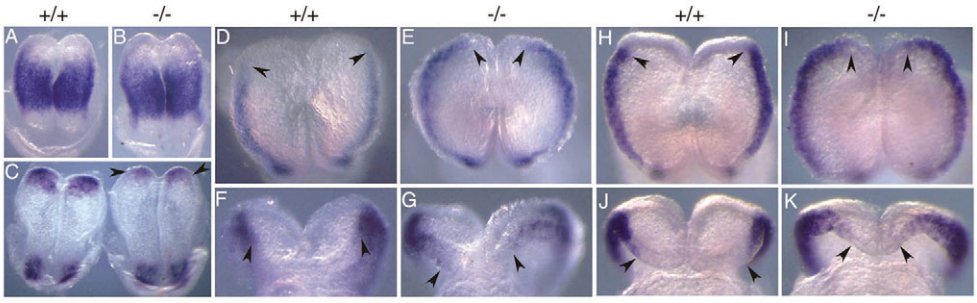

Fig. 1. Posterior transformation of the AFB in *Hesx1*$^{-/-}$ mutants at early somite stages. (**A**,**B**) Dorsal view of the *Pax2* expression domain in wild type (A) and *Hesx1*$^{-/-}$ mutant (B) at presomitic stages. No significant differences are observable. (**C**) Dorsal view of the *Pax6* expression domain in wild type (left) and *Hesx1*$^{-/-}$ mutant (right) at the 0- to 1-somite stage. Note the reduction in *Pax6* expression in the anterior NP (arrowheads). (**D-G**) Dorsal (D,E) and frontal (F,G) views of *Pax3* expression domain in wild type (D,F) and *Hesx1*$^{-/-}$ mutant (E,G) at the 2- to 3-somite stage. *Pax3* expression domain is anteriorised in the *Hesx1*$^{-/-}$ mutant (E,G). Arrowheads indicate the rostral limit of *Pax3* expression. (**H-K**) Dorsal (H,I) and frontal (J,K) views of *Foxd3* expression domain in wild type (H,J) and *Hesx1*$^{-/-}$ mutant (I,K) at the 2- to 3-somite stage. *Foxd3* expression domain is anteriorised in the *Hesx1*$^{-/-}$ mutant (I,K). Arrowheads indicate the rostral limit of *Foxd3* expression. Anterior is to the top in A-E,H,I.

cells are posterior NP derivatives that delaminate from the boundaries of the NP along the entire axis, with the exception of the most anterior neural ectoderm fated to be AFB (Couly and Le Douarin, 1987; Sechrist et al., 1995; Muhr et al., 1997). Therefore, our data suggest that the AFB loses its identity in *Hesx1*$^{-/-}$ mutants in favour of NC.

Wnt/β-catenin ectopic activation in the AFB of *Hesx1*$^{-/-}$ mutants

We analysed the expression patterns of *Wnt1* and *Fgf8* because they are essential signals required for normal expansion and patterning of midbrain and AFB, respectively (McMahon and Bradley, 1990; Echelard et al., 1994; Meyers et al., 1998; Storm et al., 2006). In the 3- to 4-somite wild-type embryo, there was a segment of the NP that expressed *Wnt1* (prospective midbrain), but the most anterior part of the NP was devoid of *Wnt1* transcripts (Fig. 2A). By contrast, in *Hesx1*$^{-/-}$ mutants, the *Wnt1* expression domain was expanded rostrally throughout the edge of the NP until its most anterior tip (Fig. 2B). This anteriorisation was not observed at earlier stages, but *Wnt1* expression is barely detectable at the 2-somite stage (Echelard et al., 1994). The onset of *Fgf8* expression in the anterior neural ridge (ANR) occurs at the 4- to 5-somite stage in wild-type embryos (Crossley and Martin, 1995; Shimamura and Rubenstein, 1997). At this stage, the *Fgf8* expression domain in the ANR was either reduced or absent in *Hesx1*-null mutants (Fig. 2C-F).

To check whether Wnt/β-catenin signalling was ectopically activated within the prospective AFB, we analysed the expression of the Wnt/β-catenin targets *Axin2* and *Sp5* (Jho et al., 2002; Takahashi et al., 2005; Weidinger et al., 2005). Normally, *Axin2* and *Sp5* are not expressed in the most anterior region of the NP of the 2- to 3-somite stage wild-type embryo (Fig. 2K,M and data not shown). Strikingly, *Axin2* expression was anteriorised in the mutants as compared with wild-type littermates at the 3- to 4-somite stage (Fig. 2G,H). Likewise, *Sp5* transcripts were detected all over the anterior NP of *Hesx1*$^{-/-}$ mutants at the 2- to 3-somite and 5- to 6-somite stages (Fig. 2I-N). Taken together, this marker analysis suggests that the lack of *Hesx1* leads to the ectopic activation of Wnt/β-catenin signalling in the prospective AFB prior to the onset of *Fgf8* expression in the ANR.

Rostral expansion of dorsal diencephalic markers in *Hesx1*$^{-/-}$ mutants

The anterior expansion of posterior neural markers was also evident in *Hesx1* mutant embryos at the 8-to 10-somite stage, although at these stages there was a marked reduction of AFB tissue. *Pax3* and *Foxd3* expression domains did not reach the most anterior region of the developing forebrain in the wild type and heterozygous *Hesx1* mutants, but did so in *Hesx1*$^{-/-}$ mutants (Fig. 3A-D) (Goulding et al., 1991; Labosky and Kaestner, 1998). *Wnt1* is normally expressed in the midbrain and posterior diencephalon, whereas *Wnt3a* is

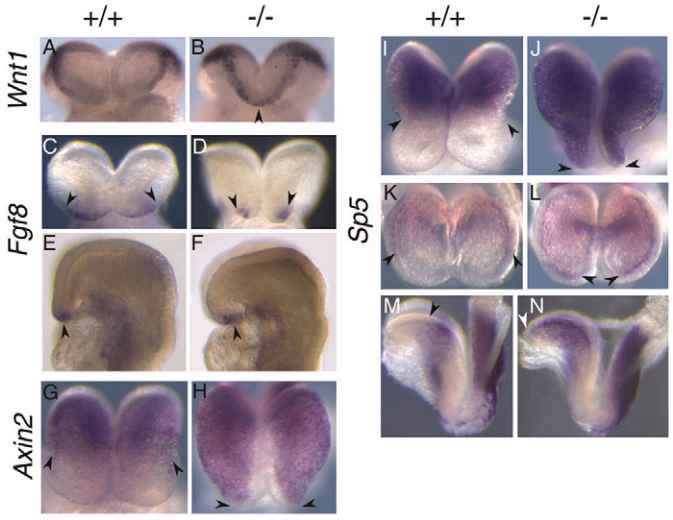

Fig. 2. Wnt/β-catenin pathway is activated in the AFB of *Hesx1*$^{-/-}$ mutants at early somite stages. (**A**,**B**) Rostral view of the *Wnt1* expression domain in wild type (A) and *Hesx1*$^{-/-}$ mutant (B) at the 3- to 4-somite stage. *Wnt1* transcripts do not reach the rostral tip of the NP in wild-type embryos, but do so in *Hesx1*$^{-/-}$ mutants (arrowhead). (**C-F**) Frontal (C,D) and lateral (E,F) views of the *Fgf8* expression domain in wild type (C,E) and *Hesx1*$^{-/-}$ mutant (D,F) at the 4- to 5-somite stage. *Fgf8* expression in the anterior neural ridge (ANR) is reduced in the *Hesx1*$^{-/-}$ mutant. Arrowheads in C,D indicate the posterior limit of the *Fgf8* expression domain in the ANR. (**G**,**H**) Expression of the Wnt/β-catenin target *Axin2* in wild type (G) and *Hesx1*$^{-/-}$ mutant (H) at the 3- to 4-somite stage. Dorsal view, anterior is to the bottom. Note the expansion of the *Axin2* expression domain in the *Hesx1*$^{-/-}$ mutant (H). Arrowheads indicate the rostral limit of *Axin2* expression. (**I-N**) Dorsal (I-L) and lateral (M,N) views of the expression domain of the Wnt/β-catenin target *Sp5* in wild type (I,K,M) and *Hesx1*$^{-/-}$ mutant (J,L,N) at the 5- to 6-somite (I,J) and the 2- to 3-somite (K-N) stages. Anterior is to the bottom (I-L) or to the left (M,N). Note the expansion of *Sp5* expression throughout the anterior NP in the *Hesx1* mutant (J,L,N). Only the most rostromedial region of the NP is free of *Sp5* transcripts (arrowheads indicate the rostral limit of *Sp5* expression).

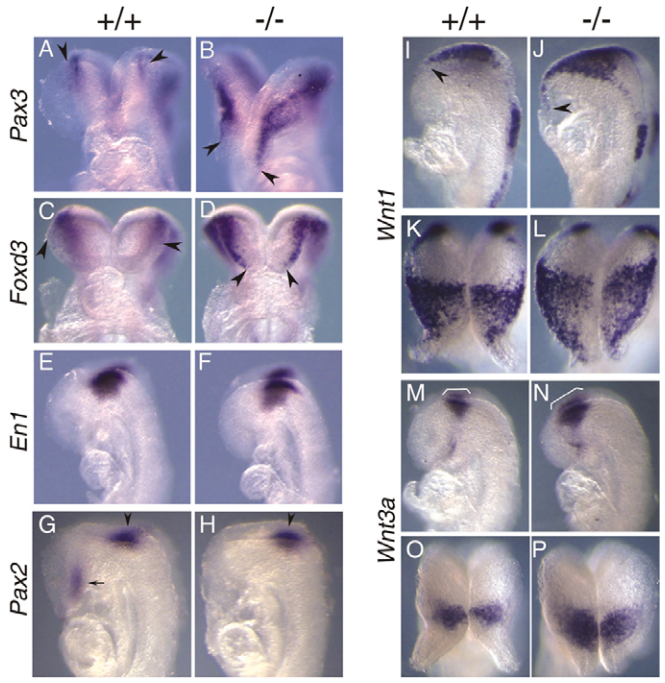

Fig. 3. Rostral expansion of dorsal diencephalic markers in *Hesx1*$^{-/-}$ mutants at the 8- to 10-somite stage. (**A-D**) Frontal views of the *Pax3* (A,B) and *Foxd3* (C,D) expression domains in wild type (A,C) and *Hesx1*$^{-/-}$ mutants (B,D). Both expression domains are anteriorised in the *Hesx1*$^{-/-}$ mutants. Arrowheads indicate the rostral limit of *Pax3* and *Foxd3* expression. (**E**,**F**) Lateral view of the *En1* expression domain in wild type (E) and *Hesx1*$^{-/-}$ mutant (F). *En1* expression domain around the midbrain-hindbrain region is normal in *Hesx1*$^{-/-}$ mutants when compared with wild-type littermates. (**G**,**H**) Lateral view of the *Pax2* expression domain in wild type (G) and *Hesx1*$^{-/-}$ mutant (H). *Pax2* expression around the midbrain-hindbrain boundary is normal (arrowheads), but there is no *Pax2* expression in the AFB of the *Hesx1*$^{-/-}$ mutant (arrow in G). (**I**,**J**) Lateral view of the *Wnt1* expression domain in wild type (I) and *Hesx1*$^{-/-}$ mutant (J). In the mutant, *Wnt1* expression is expanded rostrally until the tip of the NP (arrowhead). (**K**,**L**) Dorsal view of the embryos depicted in I,J with anterior to the bottom. (**M**,**N**) Lateral view of the *Wnt3a* expression domain in wild type (M) and *Hesx1*$^{-/-}$ mutant (N). Note the rostral expansion of *Wnt3a* expression in the prospective dorsal diencephalon (bracket). (**O**,**P**) Dorsal view of the embryos depicted in M and N with anterior to the bottom.

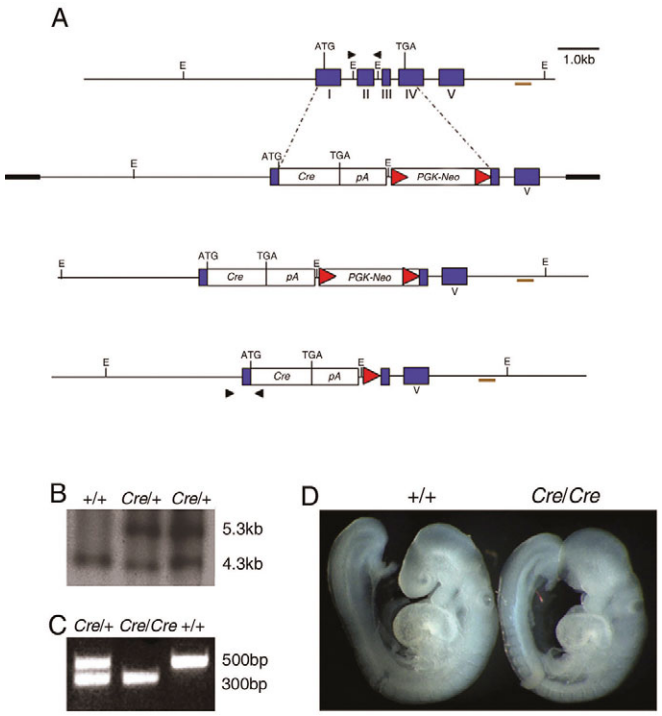

Fig. 4. Generation of the *Hesx1-Cre* targeted allele. (**A**) Top to bottom: structure of the murine *Hesx1* wild-type locus, *Hesx1-Cre* targeting vector and *Hesx1-Cre* allele prior to and after flipase excision of the *neo* cassette. The map of the targeting vector shows the replacement of the *Hesx1* coding region by a cassette containing the *Cre* recombinase gene and the neomycin resistance gene under the *PGK* promoter (*PGK-Neo*) flanked by *Frt* sites (red triangles). (**B**) Southern blot hybridisation of DNA samples from wild type (+/+) and two heterozygous (*Cre*/+) ES cell clones cut with *Eco*RI and hybridised with an external probe (brown line in A). (**C**) Representative example of PCR genotyping of DNA samples from wild-type, *Hesx1*$^{Cre/+}$ and *Hesx1*$^{Cre/Cre}$ embryos. (**D**) Wild-type embryo (left) and *Hesx1*$^{Cre/Cre}$ mutant showing lack of AFB tissue (telencephalon and eye).

expressed only in the dorsal diencephalon (Parr et al., 1993). At these stages, *Wnt1* and *Wnt3a* were also clearly anteriorised and their expression domains were enlarged (Fig. 3I-P). Therefore, the *Wnt1* and *Wnt3a* anteriorisation might reflect the transformation of AFB into posterior diencephalic fates observed at earlier stages. The expression domains of *Pax2*, *Fgf8*, *Pax6* and *Six3* in the AFB region were significantly reduced in *Hesx1*$^{-/-}$ mutants at 8.5 dpc (Fig. 3G,H and data not shown) (Nornes et al., 1990; Crossley and Martin, 1995; Walther and Gruss, 1991; Oliver et al., 1995). However, more-posterior markers, such as *En1* (a midbrain-hindbrain boundary marker) and *Hoxb1* (hindbrain marker) were unperturbed in *Hesx1*-deficient embryos (Fig. 3E,F and data not shown) (Wurst et al., 1994; Hunt and Krumlauf, 1991). At 9.5 dpc, rostral expansion of the *Atx* and *Pax6* expression domains in the posterior diencephalic region was evident in *Hesx1*$^{-/-}$ mutants (see Fig. S1A,B in the supplementary material).

A reduction in cell proliferation in the anterior NP and/or an increase in cell death might also contribute to the forebrain defects observed in *Hesx1*-deficient embryos. Proliferation and apoptosis in the NP were analysed using an anti-phosphorylated histone H3 antibody and TUNEL staining, respectively. No significant differences were observed in the mitotic indices between *Hesx1*$^{-/-}$ (4.29%) and wild-type (4.72%) embryos from 7.5 to 8.5 dpc. Likewise, cell death was negligible within the anterior NP at streak and head-fold stages and no significant differences were observed between *Hesx1*$^{-/-}$ and wild-type littermates at 8.5 dpc (see Fig. S1I-L in the supplementary material). However, at 9.5 dpc, *Hesx1*$^{-/-}$ mutants exhibited exacerbated apoptosis within neural tissue at the level of the posterior forebrain-midbrain boundary. Cell death in the roof plate of the telencephalon was reduced as compared with that in heterozygous or wild-type littermates (see Fig. S1C-F in the supplementary material). Since enhanced apoptosis occurs in a domain of the forebrain where *Hesx1* is never expressed and after the onset of forebrain defects, we conclude it is an indirect effect of the abnormal development of the forebrain in *Hesx1* mutants.

Altogether, these data indicate that the reduction of AFB tissue in *Hesx1* mutants from 8.5 dpc onwards is caused by the posteriorisation of AFB precursors at early somite stages.

Cell fate analysis of *Hesx1*-expressing cells in normal and *Hesx1*-deficient embryos

We carried out genetic fate mapping of *Hesx1*-expressing cells using a novel *Hesx1-Cre* mouse line (Fig. 4) and the *R26-floxstop-lacZ* reporter line (hereby called *R26-Cond-lacZ*) (Soriano, 1999). X-Gal staining of $Hesx1^{Cre/+};R26^{Cond\text{-}lacZ/Cond\text{-}lacZ}$ embryos, which are phenotypically normal, revealed *lacZ* expression in all cell types where *Hesx1* is normally expressed and their descendants (see Fig. S2 in the supplementary material). This analysis revealed that the normal fate of *Hesx1*-expressing cells within the NP is to colonise the AFB.

This fate analysis was also performed on *Hesx1*-deficient embryos. By comparing $Hesx1^{Cre/+};R26^{Cond\text{-}lacZ/+}$ and $Hesx1^{Cre/-};R26^{Cond\text{-}lacZ/+}$ compound embryos, differences in the fate of *lacZ*-expressing cells between genotypes could be attributed to the loss of *Hesx1*, as *Cre* and *lacZ* dosage is the same in both.

First, we analysed the *Cre* expression pattern in $Hesx1^{Cre/+}$, $Hesx1^{Cre/-}$ and $Hesx1^{Cre/Cre}$ embryos. ISH on $Hesx1^{Cre/Cre}$ embryos at 8.5 dpc revealed a pattern of *Cre* expression that was very similar to the *Hesx1* expression domain in wild-type embryos (see Fig. S3A-C in the supplementary material). No differences in *Cre* expression were observed between $Hesx1^{Cre/+}$ and $Hesx1^{Cre/-}$ embryos, although the intensity of the expression domain was weaker in embryos carrying just one copy of *Cre* (see Fig. S3D,E in the supplementary material). RT-PCR on $Hesx1^{Cre/+}$ and $Hesx1^{Cre/-}$ embryos from 7.5-9.5 dpc detected *Cre* expression at all stages analysed, but no expression was detected in the brain of 11.5-dpc embryos (data not shown). qRT-PCR revealed no differences in *Cre* expression between $Hesx1^{Cre/+}$ and $Hesx1^{Cre/-}$ embryos at the 2-somite stage, but a reduction in *Cre* expression was observed in $Hesx1^{Cre/-}$ embryos at the 5-somite stage, possibly reflecting the ongoing posterior transformation of the AFB (see Fig. S3F in the supplementary material). These data suggest that there is no ectopic expression of *Cre* within the NP of *Hesx1*-deficient embryos.

No significant differences in X-Gal staining were observed from the onset of gastrulation to the 2- to 3-somite stage between $Hesx1^{Cre/+};R26^{Cond\text{-}lacZ/+}$ and $Hesx1^{Cre/-};R26^{Cond\text{-}lacZ/+}$ embryos (see Fig. S2B and Fig. S4F in the supplementary material). However, at the 4- to 5-somite stage, X-Gal-positive cells reached more posterior regions of the NP in $Hesx1^{Cre/-};R26^{Cond\text{-}lacZ/+}$ embryos as compared with $Hesx1^{Cre/+};R26^{Cond\text{-}lacZ/+}$ littermates (Fig. 5A,B). The majority of *lacZ*-expressing cells in $Hesx1^{Cre/+};R26^{Cond\text{-}lacZ/+}$ compound embryos at the 8- to 10-somite stage remained anterior to the point of fusion between the cranial folds at the boundary between anterior and posterior forebrain (Fig. 5C). By contrast, abundant *lacZ*-expressing cells were observed posterior to this boundary in $Hesx1^{Cre/-};R26^{Cond\text{-}lacZ/+}$ mutants (Fig. 5D). These differences were accentuated at 9.5 dpc. Moreover, *lacZ*-expressing cells also colonised the first branchial arch in $Hesx1^{Cre/-};R26^{Cond\text{-}lacZ/+}$ embryos from 9.5 dpc in a manner resembling the pattern of endogenous NC migration (Fig. 5I-N). This was never observed in $Hesx1^{Cre/+};R26^{Cond\text{-}lacZ/+}$ embryos (n=52). The possibility that *lacZ*-expressing cells in the first branchial arch were migratory NC was in agreement with the rostral expansion of the NC markers *Pax3* and *Foxd3* (Fig. 1D-K and Fig. 3A-D). In fact, at 16.5 dpc, *lacZ*-expressing cells were found in skull bones, dermis, maxilar and mandibular bones, basisphenoid and vibrissae of $Hesx1^{Cre/-};R26^{Cond\text{-}lacZ/+}$ mutants, which are all tissues normally colonised by cranial NC (see Fig. S4 in the supplementary material, and data not shown) [Creuzet et al. (Creuzet et al., 2005) and references therein]. No differences in X-Gal staining were observed in the endoderm of the pharyngeal arches and the liver between the two genotypes.

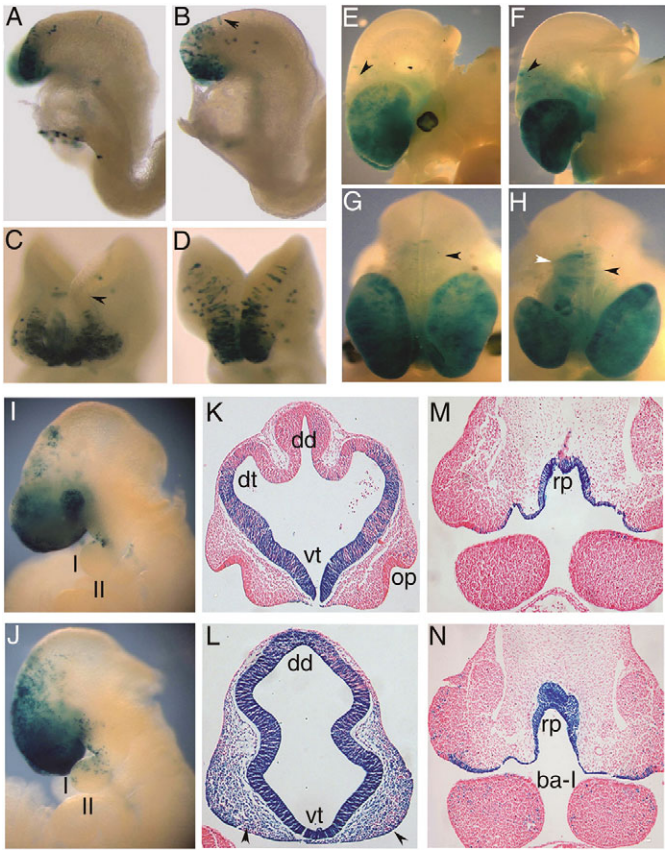

Fig. 5. Descendants of *Hesx1*-expressing cells in the anterior NP colonise posterior regions of the neural tube and the first branchial arch. All embryos were X-Gal stained. (**A**,**B**) Higher numbers of *lacZ*-expressing cells reach more posterior regions of the NP in the $Hesx1^{Cre/-};R26^{Cond\text{-}lacZ/+}$ mutant (B, arrowhead) as compared with a $Hesx1^{Cre/+};R26^{Cond\text{-}lacZ/+}$ embryo (A) at the 6- to 7-somite stage. (**C**,**D**) This is accentuated in an 8- to 10-somite $Hesx1^{Cre/-};R26^{Cond\text{-}lacZ/+}$ mutant (D) as compared with an $Hesx1^{Cre/+};R26^{Cond\text{-}lacZ/+}$ embryo (C). Arrowhead in C indicates the boundary between anterior and posterior forebrain. (**E-H**) Lateral (E,F) and dorsal (G,H) views of a $Hesx1^{Cre/+};R26^{Cond\text{-}lacZ/+}$ embryo (E,G) and a $Hesx1^{Cre/-};R26^{Cond\text{-}lacZ/+}$ mutant (F,H). The brain was partially dissected to improve X-Gal staining. *lacZ*-expressing cells barely colonise the posterior forebrain of the $Hesx1^{Cre/+};R26^{Cond\text{-}lacZ/+}$ embryo (arrowheads in E,G), but massively populate this region in the $Hesx1^{Cre/-};R26^{Cond\text{-}lacZ/+}$ mutant (black arrowheads in F,H). Note that the $Hesx1^{Cre/-};R26^{Cond\text{-}lacZ/+}$ mutant depicted in F,H shows asymmetric telencephalic development with a very small right telencephalic vesicle. This is concomitant with a more pronounced degree of colonisation of *lacZ*-expressing cells on the right side of the posterior forebrain (white arrowhead). (**I**,**J**) $Hesx1^{Cre/+};R26^{Cond\text{-}lacZ/+}$ embryo (I) and $Hesx1^{Cre/-};R26^{Cond\text{-}lacZ/+}$ mutant (J) at 9.5 dpc. Note the presence of *lacZ*-expressing cells within the first branchial arch in the $Hesx1^{Cre/-};R26^{Cond\text{-}lacZ/+}$ mutant only (J). (**K-N**) Frontal sections of a $Hesx1^{Cre/+};R26^{Cond\text{-}lacZ/+}$ embryo (K,M) and a $Hesx1^{Cre/-};R26^{Cond\text{-}lacZ/+}$ mutant (L,N) at 10.5 dpc. Many more *lacZ*-expressing cells are localised in the frontonasal mass (arrowheads in L) of the $Hesx1^{Cre/-};R26^{Cond\text{-}lacZ/+}$ mutant embryos as compared with the $Hesx1^{Cre/+};R26^{Cond\text{-}lacZ/+}$ embryo (K). *lacZ*-expressing cells within the first branchial arch are only observed in the $Hesx1^{Cre/-};R26^{Cond\text{-}lacZ/+}$ embryo. ba-I, first branchial arch; dd, dorsal diencephalon; dt, dorsal telencephalon; op, olfactory placode; rp, Rathke's pouch; vt, ventral telencephalon.

At 12.5 dpc, most of the *lacZ*-expressing cells colonised the telencephalic vesicles, eyes, hypothalamus and ventral diencephalon in the *Hesx1*$^{Cre/+}$;*R26*$^{Cond\text{-}lacZ/+}$ embryos, and only sporadic stained cells were observed within the frontonasal mass and the posterior forebrain (Fig. 5E,G). By contrast, *Hesx1*$^{Cre/-}$;*R26*$^{Cond\text{-}lacZ/+}$ embryos showed an abundance of *lacZ*-expressing cells in the posterior forebrain and frontonasal mass, in addition to the ectopic *lacZ*-expressing cells within the first branchial arch (Fig. 5F,H and data not shown). We noticed that *Hesx1*-deficient embryos at 11.5-12.5 dpc had more *lacZ*-expressing cells localised in the AFB (Fig. 5E,F). Since *Cre* expression is not activated ectopically within the NP, this finding might be due to the fact that in these embryos the AFB derives predominantly from the most rostro-medial (RM) region of the early NP, as more lateral regions change fate to posterior forebrain and NC (Figs 1 and 2). The RM region of the NP contains a higher density of *lacZ*-expressing cells than more lateral regions (see Fig. S2B and Fig. S4F in the supplementary material). By contrast, the AFB of *Hesx1*$^{Cre/+}$;*R26*$^{Cond\text{-}lacZ}$ embryos derives from regions of the early anterior NP, containing both high and low densities of *lacZ*-expressing cells.

Often, asymmetric development of the telencephalic and optic vesicles was observed in *Hesx1*$^{Cre/-}$;*R26*$^{Cond\text{-}lacZ/+}$ mutants (~75%, *n*=134), in agreement with previous observations (Dattani et al., 1998). In these embryos, one side developed better than the other, with the right side commonly being the most severely affected (95%) (Fig. 5H). The greater reduction of telencephalic and eye tissue was concomitant with an increased colonisation of X-Gal-positive cells in the posterior forebrain of the same side. This suggests that more cells that would normally colonise the telencephalon and eyes have reverted their fate to posterior forebrain in the most-affected side. The reasons underlying the asymmetry defects in *Hesx1*-deficient embryos remain unknown at present, as *Hesx1* is not expressed asymmetrically within the NP. X-Gal staining on whole brains followed by ISH with *Shh* and *Pax6* revealed that *lacZ*-expressing cells did not cross the forebrain-midbrain boundary, which is marked by the posterior limit of *Pax6* expression in the forebrain (Inoue et al., 2000) (see Fig. S5 in the supplementary material).

Taken together, these data indicate that a lack of *Hesx1* expression causes a transformation of the AFB primordium, which acquires a posterior forebrain identity and generates NC.

Hesx1 might not be sufficient to change posterior neural fates

If a lack of *Hesx1* leads to a posteriorisation of the forebrain, could *Hesx1* misexpression alter posterior fates when ectopically expressed? To address this issue we generated a *R26-Cond-Hesx1* mouse line by gene targeting in ES cells (see Fig. S6 in the supplementary material). In this mouse, *Hesx1* expression is activated upon Cre-mediated excision of the stop cassette.

R26$^{Cond\text{-}Hesx1/+}$ mice were crossed with the *β-Actin-Cre* transgenic line, in which *Cre* expression is driven by the *β-Actin* (*Actb*) promoter (Meyers et al., 1998). *R26*$^{Cond\text{-}Hesx1/+}$;*β-Actin-Cre* compound embryos expressed *Hesx1* transcripts ubiquitously (except in the heart where *β-Actin* is not active), whereas *R26*$^{Cond\text{-}Hesx1/+}$, *β-Actin-Cre* and wild-type littermates expressed *Hesx1* only within the endogenous domain in the ventral forebrain and/or Rathke's pouch (see Fig. S6D,E in the supplementary material). Western blot analysis of whole heads demonstrated that *R26*$^{Cond\text{-}Hesx1/+}$;*β-Actin-Cre* compound embryos contained more HESX1 protein than *R26*$^{Cond\text{-}Hesx1/+}$, *β-Actin-Cre* or wild-type littermates (see Fig. S6F in the supplementary material). Protein levels were even higher when embryos contained two copies of the *R26-Cond-Hesx1* allele in *R26*$^{Cond\text{-}Hesx1/Cond\text{-}Hesx1}$;*β-Actin-Cre* compound embryos (data not shown).

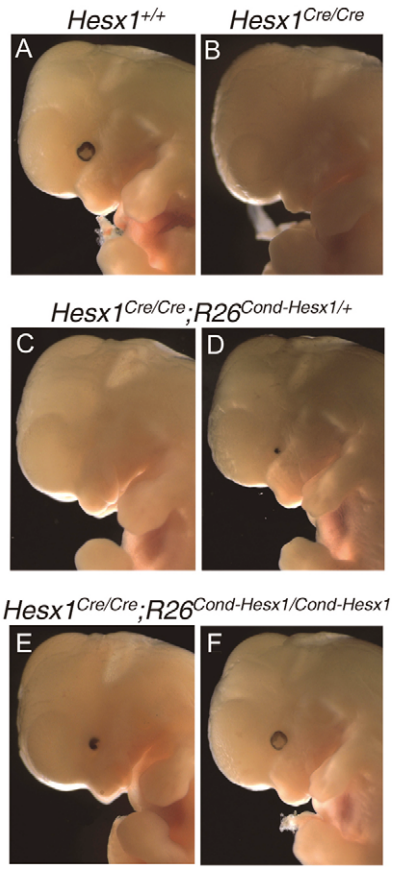

Fig. 6. Genetic rescue of the forebrain defects in the *Hesx1*-deficient embryos. (**A**,**B**) 12.5-dpc wild-type (A) and *Hesx1*$^{Cre/Cre}$ (B) embryos. Note the small telencephalic vesicle and the absence of the eye in the mutant embryo (B). (**C**,**D**) 12.5-dpc *Hesx1*$^{Cre/Cre}$;*R26*$^{Cond\text{-}Hesx1/+}$ compound embryos. Note the significant rescue of telencephalic development, but very little (D) or no rescue (C) of the eye defects. (**E**,**F**) 12.5-dpc *Hesx1*$^{Cre/Cre}$;*R26*$^{Cond\text{-}Hesx1/\ Cond\text{-}Hesx1}$ compound embryos showing significant rescue of both telencephalon and eye development.

Marker analysis revealed no significant differences in the expression of *Six3*, *Pax3*, *Foxd3*, *Wnt1* and *Fgf8* between *R26*$^{Cond\text{-}Hesx1/+}$;*β-Actin-Cre*, *R26*$^{Cond\text{-}Hesx1/Cond\text{-}Hesx1}$;*β-Actin-Cre*, single mutants and wild-type littermates (data not shown). Therefore, it seems likely that *Hesx1* is not sufficient to confer anterior identity to posterior neural tissues. However, a proportion of compound embryos overexpressing *Hesx1* had exencephaly (10% of *R26*$^{Cond\text{-}Hesx1/+}$;*β-Actin-Cre*, *n*=65; and 80% of *R26*$^{Cond\text{-}Hesx1/Cond\text{-}Hesx1}$;*β-Actin-Cre*, *n*=35) (see Fig. S6E in the supplementary material). The reasons underlying the exencephaly are at present unknown, but this phenotype is background-dependent and not detected in a mixed C57BL6/J;CD1 background (data not shown).

AFB is likely to exhibit a differential sensitivity to *Hesx1* levels

We used the *R26-Cond-Hesx1* mouse line in an attempt to rescue the forebrain defects of the *Hesx1* homozygous mutants. Controlling the *Hesx1* dosage from the *R26* locus, by adding either one or two

Table 1. Genotype of mice resulting from *Hesx1*$^{Cre/+}$;*R26*$^{Hesx1/+}$ intercrosses

Genotype	Number of embryos	
	Obtained	Expected (%)
Hesx1$^{+/+}$;*R26*$^{+/+}$	8	7-8 (6.25)
Hesx1$^{+/+}$;*R26*$^{Hesx1/+}$	23	15 (12.5)
Hesx1$^{+/+}$;*R26*$^{Hesx1/Hesx1}$	9	7-8 (6.25)
Hesx1$^{Cre/+}$;*R26*$^{+/+}$	14	15 (12.5)
Hesx1$^{Cre/+}$;*R26*$^{Hesx1/+}$	39	30 (25)
Hesx1$^{Cre/+}$;*R26*$^{Hesx1/Hesx1}$	19	15 (12.5)
Hesx1$^{Cre/Cre}$;*R26*$^{+/+}$	0	7-8 (6.25)
Hesx1$^{Cre/Cre}$;*R26*$^{Hesx1/+}$	5	15 (12.5)
Hesx1$^{Cre/Cre}$;*R26*$^{Hesx1/Hesx1}$	4	7-8 (6.25)
Total number of embryos	121	

Mice were genotyped at weaning.

copies on a *Hesx1*-null background, might reveal distinct requirements for HESX1 protein levels for normal development of specific AFB structures.

R26$^{Cond\text{-}Hesx1/Cond\text{-}Hesx1}$ homozygous animals were crossed with *Hesx1*$^{Cre/+}$ mice to generate *Hesx1*$^{Cre/+}$;*R26*$^{Cond\text{-}Hesx1/+}$ compound heterozygotes. Table 1 summarises the results of all genotypes determined at weaning in the offspring of *Hesx1*$^{Cre/+}$;*R26*$^{Cond\text{-}Hesx1/+}$ intercrosses. As expected, no *Hesx1*$^{Cre/Cre}$ animals were obtained (see Materials and methods). However, five mice of *Hesx1*$^{Cre/Cre}$;*R26*$^{Cond\text{-}Hesx1/+}$ and four mice of *Hesx1*$^{Cre/Cre}$;*R26*$^{Cond\text{-}Hesx1/Cond\text{-}Hesx1}$ genotype were identified. All exhibited eye abnormalities, except for one *Hesx1*$^{Cre/Cre}$;*R26*$^{Cond\text{-}Hesx1/Cond\text{-}Hesx1}$ mouse that had normal eyes. These data suggest that the addition of HESX1 from the *R26-Cond-Hesx1* allele can rescue the perinatal lethality observed in the *Hesx1* homozygous mutants.

To assess the degree of rescue of AFB structures, *Hesx1*$^{Cre/+}$;*R26*$^{Cond\text{-}Hesx1/+}$ mice were intercrossed and 12.5-dpc embryos were subject to morphological and histological analyses. *Hesx1*$^{Cre/Cre}$ embryos obtained from *Hesx1*$^{Cre/+}$;*R26*$^{Cond\text{-}Hesx1/+}$ intercrosses showed reduced or absent telencephalon, but eye defects were fully penetrant with variable expressivity ranging from unilateral microphthalmia to bilateral anophthalmia (n=7) (Fig. 6B) (Dattani et al., 1998). By contrast, *Hesx1*$^{Cre/Cre}$;*R26*$^{Cond\text{-}Hesx1/+}$ embryos showed a significant improvement in AFB development (Fig. 6C,D). The size and shape of the telencephalic vesicles in *Hesx1*$^{Cre/Cre}$;*R26*$^{Cond\text{-}Hesx1/+}$ embryos was comparable with wild-type littermates in nine out of 12 embryos. However, there was no major improvement in eye development. Of the embryos recovered, all had abnormal eyes (n=12), and either showed bilateral anophthalmia (n=10) or unilateral microphthalmia (n=2). Eye phenotype rescue was accentuated in *Hesx1*$^{Cre/Cre}$;*R26*$^{Cond\text{-}Hesx1/Cond\text{-}Hesx1}$ compound embryos (Fig. 6E,F). Bilateral anophthalmia was observed in only three out of ten embryos. From the remaining seven embryos, three had normal eyes, two had bilateral microphthalmia and two unilateral anophthalmia. Telencephalic development was normal in nine out of ten embryos analysed. No phenotypic defects were seen in embryos of all other genotypes. The results from these experiments allow us to draw two conclusions. First, that *Hesx1* expression from the *R26-Cond-Hesx1* allele can rescue the forebrain defects in *Hesx1*-deficient embryos. Second, that the telencephalon and eyes might exhibit a distinct sensitivity to HESX1 dosage.

The rescue of the forebrain defects was analysed at the molecular level in 8.5-dpc embryos. *Hesx1* expression was restricted to the AFB in *Hesx1*$^{Cre/Cre}$;*R26*$^{Cond\text{-}Hesx1/Cond\text{-}Hesx1}$ and wild-type

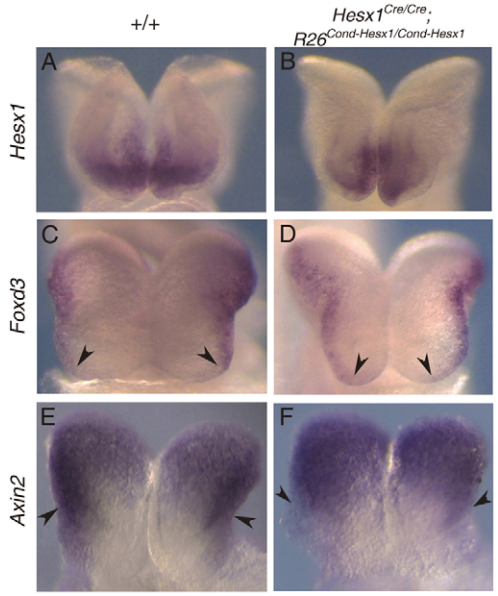

Fig. 7. AFB patterning is improved in *Hesx1*$^{Cre/Cre}$;*Rosa*$^{Cond\text{-}Hesx1/Cond\text{-}Hesx1}$ compound embryos. (**A**,**B**) Frontal view of the *Hesx1* expression domain in wild type (A) and in a *Hesx1*$^{Cre/Cre}$;Rosa$^{Cond\text{-}Hesx1/Cond\text{-}Hesx1}$ compound embryo (B), showing comparable levels of expression. (**C**,**D**) Dorsal view of *Foxd3* expression domain in wild type (C) and in a *Hesx1*$^{Cre/Cre}$;Rosa$^{Cond\text{-}Hesx1/Cond\text{-}Hesx1}$ compound embryo (D). Arrowheads indicate the region of the rostral NP where *Foxd3* is not expressed. (**E**,**F**) Frontal view of *Axin2* expression domain in wild type (E) and in a *Hesx1*$^{Cre/Cre}$;Rosa$^{Cond\text{-}Hesx1/Cond\text{-}Hesx1}$ compound embryo (F). Arrowheads indicate the rostral limit of *Axin2* expression. Note the presence of AFB tissue that is devoid of *Axin2* transcripts in E and F.

littermates and levels of expression were comparable (Fig. 7A,B). *Foxd3* expression was anteriorised in the *Hesx1*-deficient embryos (Fig. 3C,D), but the *Foxd3* expression domain in *Hesx1*$^{Cre/Cre}$;*R26*$^{Cond\text{-}Hesx1/Cond\text{-}Hesx1}$ was similar to that of wild-type embryos (Fig. 7C,D). Finally, the anteriorisation of *Axin2* expression in the *Hesx1*$^{-/-}$ mutants (Fig. 2G,H) was reverted in *Hesx1*$^{Cre/Cre}$;*R26*$^{Cond\text{-}Hesx1/Cond\text{-}Hesx1}$ compound embryos, and an *Axin2*-free region of the anterior NP was evident (Fig. 7E,F). Overall, these experiments suggest that the rescue of the morphological forebrain defects correlates with an improvement of the neural patterning of the anterior NP.

DISCUSSION

It has been previously established that *Hesx1* is essential for normal forebrain formation in mouse and humans, but the mechanisms underlying the forebrain defects of *Hesx1*-deficient embryos have remained elusive (Dattani et al., 1998; Martinez-Barbera et al., 2000). In this study we demonstrate that lack of *Hesx1* leads to a fate transformation of anterior to posterior forebrain. Cells that normally colonise the telencephalon, eyes, hypothalamus and ventral diencephalon are found in more-posterior regions, such as the dorsal thalamus and pretectum in *Hesx1*$^{-/-}$ mutants. Gain-of-function experiments indicate that *Hesx1* neither promotes AFB identity when misexpressed in the posterior NP, nor increases the size of the AFB when overexpressed in its endogenous expression domain. Moreover, our experiments suggest that the eyes might require higher levels of HESX1 protein than the telencephalon for normal

development. This study has revealed that one of the functions of *Hesx1* is to prevent the Wnt/β-catenin signalling pathway from being activated within the AFB.

Normal fate of *Hesx1*-expressing cells

The fate of *Hesx1*-expressing cells in our study is in agreement with previous fate mapping studies in the mouse. Soon after the onset of gastrulation, the anterior visceral endoderm is displaced towards the extraembryonic region by the definitive endoderm, which is formed at the tip of the primitive streak (Lawson and Pedersen, 1987; Thomas and Beddington, 1996). X-Gal staining of $Hesx1^{Cre/+};R26^{Cond\text{-}lacZ/Cond\text{-}lacZ}$ embryos detected patches of blue cells in the visceral endoderm of the extraembryonic region from late streak stages. It was noticeable that *lacZ*-expressing cells remained clumped together and, as previously described, not much intermingling was observed (Gardner and Cockroft, 1998). *Hesx1* is expressed in the axial levels of the anterior definitive endoderm, an area containing the precursors of some anterior foregut derivatives (Lawson and Pedersen, 1987; Thomas et al., 1998). In fact, *lacZ*-expressing cells colonised the anterior foregut in $Hesx1^{Cre/+};R26^{Cond\text{-}lacZ/+}$ embryos at 8.5 dpc and were found in its derivatives, including pharyngeal endoderm, thyroid gland, liver and ventral pancreas.

Strong X-Gal staining was detected in the Rathke's pouch from 9.0 dpc onwards. Interestingly, blue cells mainly colonised the anterior and intermediate lobes, both of which are derived from the oral ectoderm, but blue cells were rarely observed in the posterior pituitary, which has neural origin from a recess in the floor of the hypothalamus (see Fig. S4E in the supplementary material).

Cell fate analysis of *lacZ*-expressing cells within the NP showed that the majority of the labelled cells colonised the forebrain region anterior to the ZLI, i.e. telencephalon, eyes, hypothalamus and ventral diencephalon. Only scattered cells ended up in the dorsal thalamus and pretectum and, very rarely, *lacZ*-expressing cells crossed the forebrain-midbrain boundary. Therefore, *Hesx1* marks only prospective forebrain, in particular the AFB.

Anterior to posterior transformation of the forebrain in *Hesx1*-deficient embryos

A main finding of this study is that the absence of *Hesx1* brings about a posterior transformation of the AFB, which is evidenced by rostral expansion of the expression domains of the NC markers *Foxd3* and *Pax3*, prior to an overt morphological defect of the anterior NP. Numerous fate mapping studies have demonstrated that premigratory NC cells are dorsal cell types that form at the border of the NP, from mid-diencephalon to spinal cord levels, but not rostral to the mid-diencephalon (Couly and Le Douarin, 1987; Sechrist et al., 1995; Muhr et al., 1997). However, cells within this NC-free region can be induced to form NC when exposed to caudalising signals in explant experiments (Muhr et al., 1997). We believe that the *Hesx1* expression domain in the anterior NP corresponds to this crest-free area. For instance, X-Gal staining of $Hesx1^{Cre/+};R26^{Cond\text{-}lacZ/+}$ embryos, which are phenotypically normal, showed that the majority of *lacZ*-expressing cells colonised the AFB and did not form NC. By contrast, *lacZ*-expressing cells populated the posterior forebrain in $Hesx1^{Cre/-};R26^{Cond\text{-}lacZ/+}$ mutants, thus reaching the area of the NP that yields migratory NC of the first branchial arch and the frontonasal mass (Inoue et al., 2000; Creuzet et al., 2005).

The expression domains of *Wnt3a*, *Wnt1*, *Atx* and *Pax6* were expanded rostrally and *lacZ*-expressing cells were found throughout the dorsoventral axis of the dorsal thalamus and pretectum. This suggests that in the absence of *Hesx1*, cells initially specified to AFB fates colonise the entire segment of the posterior forebrain, not only NC-generating regions. However, the size of the posterior forebrain is not affected in *Hesx1*-deficient embryos at 12.5-18.5 dpc, possibly because the increased cell death in the posterior forebrain compensates for the excess of cells populating this region.

Although required for the maintenance of AFB identity, *Hesx1* cannot alter posterior fates in caudal neural tissue when misexpressed in the mouse embryo. To do so, *Hesx1* might require specific co-factors only present in anterior and not posterior neural tissue. (see Fig. S6 in the supplementary material) (Ermakova et al., 1999). The partial rescue of the forebrain defects and attenuation of the posterior transformation observed in $Hesx1^{Cre/Cre};R26^{Cond\text{-}Hesx1/+}$ and $Hesx1^{Cre/Cre};R26^{Cond\text{-}Hesx1/Cond\text{-}Hesx1}$ compound embryos suggest that only the AFB is competent to respond to HESX1. Overall, these data indicate that *Hesx1* is required for AFB development but, on its own, it is not sufficient to promote AFB fates.

The genetic rescue experiments have revealed that whereas one copy of *R26-Cond-Hesx1* in a *Hesx1*-null background is sufficient to improve telencephalic development, two copies of the *R26-Cond-Hesx1* allele are required to rescue both telencephalon and eye development. Although we cannot rule out the possibility that telencephalic and eye precursors could express different levels of *Hesx1* from the *R26* locus, we think that our experiments point to a differential sensitivity of the eye and telencephalon to *Hesx1* levels. Fate mapping studies in the mouse embryo have shown that telencephalic precursors reside in the rostrolateral regions of the anterior NP and that the eye field is located caudal to this and more medially (Inoue et al., 2000). It is worth noting that *Hesx1* expression is higher in the area of the NP that is thought to correspond to the eye field (Thomas and Beddington, 1996). In this scenario, eye development is expected to be more sensitive than telencephalic development to HESX1 levels, and indeed, *Hesx1*-deficient embryos show a higher penetrance of eye versus telencephalic abnormalities. In agreement with this concept, mutant mice bearing a single amino acid change in position 26 that yields a HESX1 protein with reduced repressing activity (Carvalho et al., 2003), display eye abnormalities but have normal telencephalic development (our unpublished results). This suggests that *Hesx1* might have a dual role within the anterior NP: to promote anterior versus posterior forebrain development and to segregate telencephalic and eye field identities (Stigloher et al., 2006; Mathers et al., 1997).

Hesx1 antagonises caudalising signals within the NP

Our data strongly suggest that the mechanism underlying the posterior transformation of $Hesx1^{-/-}$ mutants is the ectopic activation of Wnt/β-catenin signalling within the prospective AFB at early somite stages. Experiments in *Xenopus* and zebrafish have indicated that the eye is the most sensitive region of the NP to Wnt/β-catenin activation (Fredieu et al., 1997; van de Water et al., 2001). When zebrafish embryos were exposed for a short time to LiCl, an inhibitor of Gsk3β that enhances Wnt/β-catenin signalling, only eye development was disrupted and the treated embryos displayed microphthalmia or anophthalmia. However, when embryos were treated with LiCl for longer, they developed telencephalic as well as eye defects. An excess of Wnt/β-catenin signalling might explain the reduction in the AFB markers *Six3* and *Pax6* and the concomitant rostral expansion of the NC markers *Pax3* and *Foxd3*.

It seems likely that *Hesx1* and *Six3* might work in parallel in the maintenance of AFB identity, but through distinct mechanisms. *Hesx1* can bind to *Wnt1* regulatory elements in in-vitro assays, but

it cannot repress reporter vectors containing *Wnt1* regulatory elements (see Fig. S7 in the supplementary material). Moreover, expansion of the *Sp5* expression domain occurs prior to *Wnt1* rostralisation in *Hesx1*$^{-/-}$ mutants. Therefore, in contrast to the *Six3*$^{-/-}$ mutants, ectopic *Wnt1* expression within the prospective AFB might not be the primary reason for the forebrain defects; rather, the excess of *Wnt1* might contribute to the final morphological defects later in development.

The possibility exists that *Hesx1* may antagonise Wnt/β-catenin signalling by modulating the activity of some component(s) of the pathway causing a cell-autonomous inhibition within *Hesx1*-expressing cells. Alternatively, or in addition, *Hesx1* might repress one or more Wnt/β-catenin target genes directly, thus preventing the acquisition of posterior fates. Chimeric experiments suggest that *Hesx1* is required cell-autonomously within the NP (Martinez-Barbera et al., 2000). However, *Hesx1* function can be partially compensated for, as most *Hesx1*$^{-/-}$ mutants show some AFB development. Moreover, in chimeric embryos, *Hesx1*-deficient cells, as well as wild-type cells, can also colonise the AFB. The possibility exists that a subset of *Hesx1*$^{-/-}$ cells might be more susceptible to respond to Wnt/β-catenin signalling and acquire a posterior fate, but this might be difficult to observe in chimeric embryos, where the bulk of wild-type cells can colonise the same regions of the neural tube (Martinez-Barbera et al., 2000). Notably, the forebrain defects were completely rescued only in embryos with a high degree of chimerism, and the AFB was mainly populated with wild-type cells (Martinez-Barbera et al., 2000). Future research will elucidate the molecular function of *Hesx1*.

We are grateful to A. Copp and A. Stoker for comments on the manuscript; to A. McMahon, G. Martin, P. Gruss, F. Constantini, R. Krumlauf, A Joyner, A. Lumsden and the MRC Geneservice for probes. We thank G. Martin, P. Soriano and S. Dymecky for sharing mouse lines. This work was supported by The Wellcome Trust.

Supplementary material

Supplementary material for this article is available at http://dev.biologists.org/cgi/content/full/134/8/1499/DC1

References

Brickman, J. M., Clements, M., Tyrell, R., McNay, D., Woods, K., Warner, J., Stewart, A., Beddington, R. S. and Dattani, M. T. (2001). Molecular effects of novel mutations in *Hesx1/HESX1* associated with human pituitary disorders. *Development* **128**, 5189-5199.

Carvalho, L. R., Woods, K. S., Mendonca, B. B., Marcal, N., Zamparini, A. L., Stifani, S., Brickman, J. M., Arnhold, I. J. and Dattani, M. T. (2003). A homozygous mutation in *HESX1* is associated with evolving hypopituitarism due to impaired repressor-corepressor interaction. *J. Clin. Invest.* **112**, 1192-1201.

Couly, G. F. and Le Douarin, N. M. (1987). Mapping of the early neural primordium in quail-chick chimeras. II. The prosencephalic neural plate and neural folds: implications for the genesis of cephalic human congenital abnormalities. *Dev. Biol.* **120**, 198-214.

Creuzet, S., Couly, G. and Le Douarin, N. M. (2005). Patterning the neural crest derivatives during development of the vertebrate head: insights from avian studies. *J. Anat.* **207**, 447-459.

Crossley, P. H. and Martin, G. R. (1995). The mouse *Fgf8* gene encodes a family of polypeptides and is expressed in regions that direct outgrowth and patterning in the developing embryo. *Development* **121**, 439-451.

Dasen, J. S., Barbera, J. P., Herman, T. S., Connell, S. O., Olson, L., Ju, B., Tollkuhn, J., Baek, S. H., Rose, D. W. and Rosenfeld, M. G. (2001). Temporal regulation of a paired-like homeodomain repressor/TLE corepressor complex and a related activator is required for pituitary organogenesis. *Genes Dev.* **15**, 3193-3207.

Dattani, M. T. (2004). Novel insights into the aetiology and pathogenesis of hypopituitarism. *Horm. Res.* **62** Suppl. 3, 1-13.

Dattani, M. T., Martinez-Barbera, J. P., Thomas, P. Q., Brickman, J. M., Gupta, R., Martensson, I. L., Toresson, H., Fox, M., Wales, J. K., Hindmarsh, P. C. et al. (1998). Mutations in the homeobox gene *HESX1/Hesx1* associated with septo-optic dysplasia in human and mouse. *Nat. Genet.* **19**, 125-133.

Echelard, Y., Vassileva, G. and McMahon, A. P. (1994). Cis-acting regulatory sequences governing Wnt-1 expression in the developing mouse CNS. *Development* **120**, 2213-2224.

Ermakova, G. V., Alexandrova, E. M., Kazanskaya, O. V., Vasiliev, O. L., Smith, M. W. and Zaraisky, A. G. (1999). The homeobox gene, Xanf-1, can control both neural differentiation and patterning in the presumptive anterior neurectoderm of the *Xenopus* laevis embryo. *Development* **126**, 4513-4523.

Fredieu, J. R., Cui, Y., Maier, D., Danilchik, M. V. and Christian, J. L. (1997). Xwnt-8 and lithium can act upon either dorsal mesodermal or neurectodermal cells to cause a loss of forebrain in *Xenopus* embryos. *Dev. Biol.* **186**, 100-114.

Garcia-Castro, M. I., Marcelle, C. and Bronner-Fraser, M. (2002). Ectodermal Wnt function as a neural crest inducer. *Science* **297**, 848-851.

Gardner, R. L. and Cockcroft, D. L. (1998). Complete dissipation of coherent clonal growth occurs before gastrulation in mouse epiblast. *Development* **125**, 2397-2402.

Glinka, A., Wu, W., Delius, H., Monaghan, A. P., Blumenstock, C. and Niehrs, C. (1998). Dickkopf-1 is a member of a new family of secreted proteins and functions in head induction. *Nature* **391**, 357-362.

Gogoi, R. N., Schubert, F. R., Martinez-Barbera, J. P., Acampora, D., Simeone, A. and Lumsden, A. (2002). The paired-type homeobox gene Dmbx1 marks the midbrain and pretectum. *Mech. Dev.* **114**, 213-217.

Goulding, M. D., Chalepakis, G., Deutsch, U., Erselius, J. R. and Gruss, P. (1991). Pax-3, a novel murine DNA binding protein expressed during early neurogenesis. *EMBO J.* **10**, 1135-1147.

Heisenberg, C. P., Houart, C., Take-Uchi, M., Rauch, G. J., Young, N., Coutinho, P., Masai, I., Caneparo, L., Concha, M. L., Geisler, R. et al. (2001). A mutation in the Gsk3-binding domain of zebrafish Masterblind/Axin1 leads to a fate transformation of telencephalon and eyes to diencephalon. *Genes Dev.* **15**, 1427-1434.

Hermesz, E., Mackem, S. and Mahon, K. A. (1996). Rpx: a novel anterior-restricted homeobox gene progressively activated in the prechordal plate, anterior neural plate and Rathke's pouch of the mouse embryo. *Development* **122**, 41-52.

Houart, C., Caneparo, L., Heisenberg, C., Barth, K., Take-Uchi, M. and Wilson, S. (2002). Establishment of the telencephalon during gastrulation by local antagonism of Wnt signaling. *Neuron* **35**, 255-265.

Hsieh, J. C., Kodjabachian, L., Rebbert, M. L., Rattner, A., Smallwood, P. M., Samos, C. H., Nusse, R., Dawid, I. B. and Nathans, J. (1999). A new secreted protein that binds to Wnt proteins and inhibits their activities. *Nature* **398**, 431-436.

Hunt, P. and Krumlauf, R. (1991). Deciphering the Hox code: clues to patterning branchial regions of the head. *Cell* **66**, 1075-1078.

Inoue, T., Nakamura, S. and Osumi, N. (2000). Fate mapping of the mouse prosencephalic neural plate. *Dev. Biol.* **219**, 373-383.

Ivanova, A., Signore, M., Caro, N., Greene, N. D. E., Copp, A. J. and Martinez-Barbera, J. P. (2005). *In vivo* genetic ablation by Cre-mediated expression of diphtheria toxin fragment A. *Genesis* **43**, 129-135.

Jho, E. H., Zhang, T., Domon, C., Joo, C. K., Freund, J. N. and Costantini, F. (2002). Wnt/β-catenin/Tcf signaling induces the transcription of Axin2, a negative regulator of the signaling pathway. *Mol. Cell. Biol.* **22**, 1172-1183.

Kazanskaya, O. V., Severtzova, E. A., Barth, K. A., Ermakova, G. V., Lukyanov, S. A., Benyumov, A. O., Pannese, M., Boncinelli, E., Wilson, S. W. and Zaraisky, A. G. (1997). Anf: a novel class of vertebrate homeobox genes expressed at the anterior end of the main embryonic axis. *Gene* **200**, 25-34.

Kiecker, C. and Niehrs, C. (2001). A morphogen gradient of Wnt/β-catenin signalling regulates anteroposterior neural patterning in *Xenopus*. *Development* **128**, 4189-4201.

Kim, C. H., Oda, T., Itoh, M., Jiang, D., Artinger, K. B., Chandrasekharappa, S. C., Driever, W. and Chitnis, A. B. (2000). Repressor activity of Headless/Tcf3 is essential for vertebrate head formation. *Nature* **407**, 913-916.

Kimura, C., Yoshinaga, K., Tian, E., Suzuki, M., Aizawa, S. and Matsuo, I. (2000). Visceral endoderm mediates forebrain development by suppressing posteriorizing signals. *Dev. Biol.* **225**, 304-321.

Knoetgen, H., Teichmann, U. and Kessel, M. (1999). Head-organizing activities of endodermal tissues in vertebrates. *Cell. Mol. Biol. Noisy-le-grand* **45**, 481-492.

Kudoh, T., Wilson, S. W. and Dawid, I. B. (2002). Distinct roles for Fgf, Wnt and retinoic acid in posteriorizing the neural ectoderm. *Development* **129**, 4335-4346.

Labosky, P. A. and Kaestner, K. H. (1998). The winged helix transcription factor Hfh2 is expressed in neural crest and spinal cord during mouse development. *Mech. Dev.* **76**, 185-190.

Lagutin, O. V., Zhu, C. C., Kobayashi, D., Topczewski, J., Shimamura, K., Puelles, L., Russell, H. R., McKinnon, P. J., Solnica-Krezel, L. and Oliver, G. (2003). *Six3* repression of Wnt signaling in the anterior neuroectoderm is essential for vertebrate forebrain development. *Genes Dev.* **17**, 368-379.

Lawson, K. A. and Pedersen, R. A. (1987). Cell fate, morphogenetic movement and population kinetics of embryonic endoderm at the time of germ layer formation in the mouse. *Development* **101**, 627-652.

Leyns, L., Bouwmeester, T., Kim, S. H., Piccolo, S. and De Robertis, E. M. (1997). Frzb-1 is a secreted antagonist of Wnt signaling expressed in the Spemann organizer. *Cell* **88**, 747-756.

Marikawa, Y. (2006). Wnt/β-catenin signaling and body plan formation in mouse embryos. *Semin. Cell Dev. Biol.* **17**, 175-184.
Martinez-Barbera, J. P., Rodriguez, T. A. and Beddington, R. S. (2000). The homeobox gene *Hesx1* is required in the anterior neural ectoderm for normal forebrain formation. *Dev. Biol.* **223**, 422-430.
Martinez-Barbera, J. P., Rodriguez, T. A., Greene, N. D. E., Weninger, W. J., Simeone, A., Copp, A. J., Beddington, R. S. P. and Dunwoodie, S. (2002). Folic acid prevents exencephaly in Cited2 deficient mice. *Hum. Mol. Genet.* **11**, 283-293.
Mathers, P. H., Grinberg, A., Mahon, K. A. and Jamrich, M. (1997). The Rx homeobox gene is essential for vertebrate eye development. *Nature* **387**, 603-607.
McMahon, A. P. and Bradley, A. (1990). The Wnt-1 (int-1) proto-oncogene is required for development of a large region of the mouse brain. *Cell* **62**, 1073-1085.
Meyers, E. N., Lewandoski, M. and Martin, G. R. (1998). An *Fgf8* mutant allelic series generated by Cre- and Flp-mediated recombination. *Nat. Genet.* **18**, 136-141.
Muhr, J., Jessell, T. M. and Edlund, T. (1997). Assignment of early caudal identity to neural plate cells by a signal from caudal paraxial mesoderm. *Neuron* **19**, 487-502.
Mukhopadhyay, M., Shtrom, S., Rodriguez-Esteban, C., Chen, L., Tsukui, T., Gomer, L., Dorward, D. W., Glinka, A., Grinberg, A., Huang, S. P. et al. (2001). Dickkopf1 is required for embryonic head induction and limb morphogenesis in the mouse. *Dev. Cell* **1**, 423-434.
Nordstrom, U., Jessell, T. M. and Edlund, T. (2002). Progressive induction of caudal neural character by graded Wnt signaling. *Nat. Neurosci.* **5**, 525-532.
Nornes, H. O., Dressler, G. R., Knapik, E. W., Deutsch, U. and Gruss, P. (1990). Spatially and temporally restricted expression of *Pax2* during murine neurogenesis. *Development* **109**, 797-809.
Oliver, G., Mailhos, A., Wehr, R., Copeland, N. G., Jenkins, N. A. and Gruss, P. (1995). *Six3*, a murine homologue of the sine oculis gene, demarcates the most anterior border of the developing neural plate and is expressed during eye development. *Development* **121**, 4045-4055.
Parr, B. A., Shea, M. J., Vassileva, G. and McMahon, A. P. (1993). Mouse Wnt genes exhibit discrete domains of expression in the early embryonic CNS and limb buds. *Development* **119**, 247-261.
Perea-Gomez, A., Rhinn, M. and Ang, S. L. (2001). Role of the anterior visceral endoderm in restricting posterior signals in the mouse embryo. *Int. J. Dev. Biol.* **45**, 311-320.
Popperl, H., Schmidt, C., Wilson, V., Hume, C. R., Dodd, J., Krumlauf, R. and Beddington, R. S. P. (1997). Misexpression of Cwnt8C in the mouse induces an ectopic embryonic axis and causes a truncation of the anterior neuroectoderm. *Development* **124**, 2997-3005.
Rodriguez, C. I., Buchholz, F., Galloway, J., Sequerra, R., Kasper, J., Ayala, R., Stewart, A. F. and Dymecky, S. M. (2000). High-efficiency deleter mice show that FLPe is an alternative to Cre-*loxP*. *Nat. Genet.* **25**, 139-140.
Satoh, K., Kasai, M., Ishidao, T., Tago, K., Ohwada, S., Hasegawa, Y., Senda, T., Takada, S., Nada, S., Nakamura, T. et al. (2004). Anteriorization of neural fate by inhibitor of β-catenin and T cell factor (ICAT), a negative regulator of Wnt signaling. *Proc. Natl. Acad. Sci. USA* **101**, 8017-8021.
Sechrist, J., Nieto, M. A., Zamanian, R. T. and Bronner-Fraser, M. (1995). Regulative response of the cranial neural tube after neural fold ablation: spatiotemporal nature of neural crest regeneration and up-regulation of Slug. *Development* **121**, 4103-4115.
Shimamura, K. and Rubenstein, J. L. (1997). Inductive interactions direct early regionalization of the mouse forebrain. *Development* **124**, 2709-2718.
Sobrier, M. L., Maghnie, M., Vie-Luton, M. P., Secco, A., di Iorgi, N., Lorini, R. and Amselem, S. (2006). Novel *HESX1* mutations associated with a life-threatening neonatal phenotype, pituitary aplasia, but normally located posterior pituitary and no optic nerve abnormalities. *J. Clin. Endocrinol. Metab.* **91**, 4528-4536.
Soriano, P. (1999). Generalized *lacZ* expression with the ROSA26 Cre reporter strain. *Nat. Genet.* **21**, 70-71.
Srinivas, S., Watanabe, T., Lin, C. S., William, C. M., Tanabe, Y., Jessell, T. M. and Costantini, F. (2001). Cre reporter strains produced by targeted insertion of EYFP and ECFP into the ROSA26 locus. *BMC Dev. Biol.* **1**, 4.
Stern, C. D. (2005). Neural induction: old problem, new findings, yet more questions. *Development* **132**, 2007-2021.
Stigloher, C., Ninkovic, J., Laplante, M., Geling, A., Tannhauser, B., Topp, S., Kikuta, H., Becker, T. S., Houart, C. and Bally-Cuif, L. (2006). Segregation of telencephalic and eye-field identities inside the zebrafish forebrain territory is controlled by Rx3. *Development* **133**, 2925-2935.
Storm, E. E., Garel, S., Borello, U., Hebert, J. M., Martinez, S., McConnell, S. K., Martin, G. R. and Rubenstein, J. L. (2006). Dose-dependent functions of *Fgf8* in regulating telencephalic patterning centers. *Development* **133**, 1831-1844.
Takahashi, M., Nakamura, Y., Obama, K. and Furukawa, Y. (2005). Identification of *SP5* as a downstream gene of the β-catenin/Tcf pathway and its enhanced expression in human colon cancer. *Int. J. Oncol.* **27**, 1483-1487.
Thomas, P. and Beddington, R. S. P. (1996). Anterior primitive endoderm may be responsible for patterning the anterior neural plate in the mouse embryo. *Curr. Biol.* **6**, 1487-1496.
Thomas, P. Q., Johnson, B. V., Rathjen, J. and Rathjen, P. D. (1995). Sequence, genomic organization, and expression of the novel homeobox gene *Hesx1*. *J. Biol. Chem.* **270**, 3869-3875.
Thomas, P. Q., Brown, A. and Beddington, R. S. (1998). Hex: a homeobox gene revealing peri-implantation asymmetry in the mouse embryo and an early transient marker of endothelial cell precursors. *Development* **125**, 85-94.
van de Water, S., van de Watering, M., Joore, J., Esseling, J., Bink, R., Clevers, H. and Zivkovic, D. (2001). Ectopic Wnt signal determines the eyeless phenotype of zebrafish masterblind mutant. *Development* **128**, 3877-3888.
Walther, C. and Gruss, P. (1991). Pax-6, a murine paired box gene, is expressed in the developing CNS. *Development* **113**, 1435-1449.
Weidinger, G., Thorpe, C. J., Wuennenberg-Stapleton, K., Ngai, J. and Moon, R. T. (2005). The Sp1-related transcription factors *Sp5* and sp5-like act downstream of Wnt/β-catenin signaling in mesoderm and neuroectoderm patterning. *Curr. Biol.* **15**, 489-500.
Wilson, S. W. and Houart, C. (2004). Early steps in the development of the forebrain. *Dev. Cell* **6**, 167-181.
Wurst, W., Auerbach, A. B. and Joyner, A. L. (1994). Multiple developmental defects in Engrailed-1 mutant mice: an early mid-hindbrain deletion and patterning defects in forelimbs and sternum. *Development* **120**, 2065-2075.
Yamaguchi, T. P. (2001). Heads or tails: Wnts and anterior-posterior patterning. *Curr. Biol.* **11**, R713-R724.